Journal of ELECTRONIC MATERIALS, Vol. 45, No. 6, 2016
DOI: 10.1007/s11664-016-4377-9

Equilibrium Lattice Relaxation and Misfit Dislocations in Step-Graded $In_xGa_{1-x}As/GaAs$ (001) and $In_xAl_{1-x}As/GaAs$ (001) Metamorphic Buffer Layers

TEDI KUJOFSA[1,2,3] and JOHN E. AYERS[1]

1.—Electrical and Computer Engineering Department, University of Connecticut, 371 Fairfield Way, Unit 4157, Storrs, CT 06269-4157, USA. 2.—e-mail: Tedi.Kujofsa@gmail.com. 3.—e-mail: Tedi.Kujofsa@engr.uconn.edu

The inclusion of metamorphic buffer layers (MBLs) in the design of lattice-mismatched semiconductor heterostructures is important in enhancing reliability and performance of optoelectronic and electronic devices through proper control of threading dislocations; threading dislocation can be reduced by allowing the distribution of the misfit dislocations throughout the MBL, rather than concentrating them at the interface where substrate defects and tangling can pin dislocations or otherwise reduce their mobility. Compositionally graded layers have been particularly used for this purpose and in this work we considered heterostructures involving a step-graded $In_xGa_{1-x}As$ or $In_xAl_{1-x}As$ epitaxial layer on a GaAs (001) substrate. For each structure type, we present minimum energy calculations including (i) the surface and (ii) average in-plane strain and (iii) the misfit dislocation density profile with various grading coefficients (thickness and indium composition variation). In both types of structures, the average in-plane strain and misfit dislocation density profile scale with the average grading coefficient, but $In_xAl_{1-x}As$ structures with a greater average elastic stiffness constants exhibit slightly higher average compressive in-plane strain (absolute valued) which is associated with higher misfit dislocation densities. However, the rate of change in the normalized relaxation percentage per unit thickness of each step with respect to the lattice mismatch of the step is lower in the $In_xAl_{1-x}As$ material system. The difference of the in-plane strain is small ($<3\%$), however, so that these material systems are virtually interchangeable in terms of their mechanical behavior ($<5.1\%$ change in elastic constants).

Key words: Relaxation, misfit dislocations, in-plane strain, step-graded, InGaAs, InAlAs, GaAs

INTRODUCTION

Metamorphic or partly relaxed semiconductor devices are of great interest because their use removes the compositional constraints associated with pseudomorphic design, enabling the use of lattice-mismatched materials with a wide range of desirable properties such as energy gap, low-field mobility and carrier saturation velocity. The realization of semiconductor heterostructures on lattice-mismatched wafers, such as strain-engineered $In_xGa_{1-x}As$ and $In_xAl_{1-x}As$ on GaAs substrate, has become critical for the fabrication of electronic and optical devices. These applications require growth of metamorphic (partly relaxed) structures with compositionally graded buffer layers to accommodate the strain associated with the mismatch between the substrate and epilayer. The graded layer allows for the introduction and distribution of misfit dislocations (MDs) away from the substrate interface which results in the reduction of

(Received March 7, 2015; accepted February 1, 2016; published online February 18, 2016)

the dislocation–dislocation interactions with substrate-associated defects; such interactions may give rise to dislocation pinning and, therefore, render threading dislocations immobile. Therefore, the enhancement of dislocation mobility from the use of a compositionally graded layer, allows for devices with reduced threading dislocation densities. In addition, the graded layer has a greater built-in residual strain near the surface which can reduce the density of threading defects by enhancing the glide velocities of dislocations, yielding the longest possible misfit segment parallel to the interface and, therefore, the least number of threading dislocations emanating from misfit dislocation ends. Although metamorphic growth has been exploited in a variety of devices,[1–10] most designs employ a linearly graded[11,12] or step-graded buffer layer.[9,13,14] Unlike a linearly graded buffer, there has been relatively little modeling work on step-graded layers and, therefore, its relaxation behavior is not well understood, but some important aspects regarding their dislocation and strain distributions have been shown experimentally. It is, therefore, worthwhile to compare the two material systems ($In_xGa_{1-x}As$ and $In_xAl_{1-x}As$) utilizing a step-graded scheme in terms of their equilibrium relaxation behavior. Equilibrium modeling in turn serves as the starting point for the understanding of kinetically limited relaxation and its results may be helpful in the optimized design of compositionally graded heterostructures.

EQUILIBRIUM MODEL

In this work, we consider $In_xGa_{1-x}As$ and $In_xAl_{1-x}As$ step-graded buffers grown on a GaAs substrate with (001) crystal orientation. The lattice mismatch is defined as $f(z) \equiv (a_s - a(z))/a(z)$, where a_s is the relaxed lattice constant of the substrate and $a(z)$ is the relaxed lattice constant of the epitaxial crystal at a distance z from the substrate interface. Step-graded layers contain a set of n uniform layers in which there are equal compositional changes from one layer to the next ("linear step grading"). For the structures studied here, the grading profile is composed of ten uniform buffer layers where the indium composition in the buffer layer is varied with a uniform step size of $\frac{1}{10}x_h$ to a final surface composition x_h corresponding to a lattice mismatch of f_h. We have investigated structures with thicknesses of 250 nm, 500 nm and 1000 nm. The material constants used in this work are summarized in Table I.

In a structure with arbitrary compositional grading profile, the equilibrium configuration may be found by applying the semiconductor heterostructure generalized energy minimization (SH-GEM) approach described by Bertoli et al.,[15] which will be summarized briefly here. In a partly relaxed layer containing misfit dislocations of cross-sectional density $\rho(z)$, the strain energy per unit area is

$$E_\varepsilon = \int_0^h Y\varepsilon_{||}^2 \mathrm{d}z = \int_0^h Y\left[f(z) + b'\int_0^z \rho_A(\zeta)\mathrm{d}\zeta\right]^2 \mathrm{d}z. \quad (1)$$

where b' is the misfit-relieving component of the Burgers vector parallel to the interface, $b' = \pm b \sin\alpha\cos\lambda$, Y is the biaxial modulus, $Y = C_{11} + C_{12} - 2C_{12}^2/C_{11}$, C_{11} and C_{12} are the elastic stiffness constants, and ζ is a variable of integration. The misfit dislocation density ρ is always positive, but b' may be positive or negative, depending on the sign of the mismatch strain (tensile or compressive) which is being relieved. The line energy of dislocations per unit area, assuming two orthogonal networks with equal cross-sectional density, is

$$E_d = 2\int_0^h F_d(z)\rho_A(z)\mathrm{d}z. \quad (2)$$

where $F_d(z)$ is the line tension of the dislocation at a distance z from the substrate interface. The equilibrium configuration may be determined numerically by minimizing $E_d + E_\varepsilon$.

RESULTS AND DISCUSSION

The $In_xGa_{1-x}As$ and $In_xAl_{1-x}As$ structures considered in this work have an ending lattice mismatch ranging from f_h = 0.8–3.4% and the two material systems were compared using identical indium composition profiles. Figure 1a shows the equilibrium misfit dislocation density profiles for 500-nm thick $In_xGa_{1-x}As$ layers on a GaAs (001) substrate with various ending indium compositions.

Table I. Material properties for InAs, AlAs, GaAs and the alloys $In_xGa_{1-x}As$ and $In_xAl_{1-x}As$

	Parameter		
Material	***a* (nm)**	**C11 (GPa)**	**C12 (GPa)**
InAs	0.50584	83.3	45.3
AlAs	0.5660	125	53.4
GaAs	0.56534	118.4	53.7
$In_xGa_{1-x}As$	0.56534 + x(0.0405)	118.4 − x(35.1)	53.7 − x(8.4)
$In_xAl_{1-x}As$	0.5660 + x(0.06016)	125 − x(41.7)	53.4 − x(8.1)

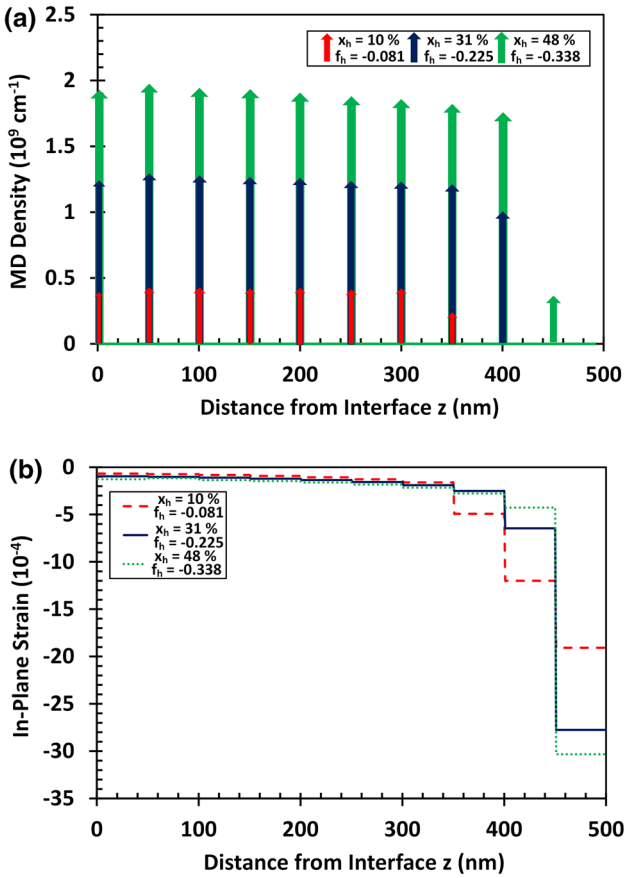

Fig. 1. (a) Misfit dislocation and (b) in-plane strain as a function of the distance from the interface with various ending compositions for step-graded $In_xGa_{1-x}As/GaAs$ and $In_xAl_{1-x}As/GaAs$ heterostructures.

In uniform layers, misfit dislocations are introduced at the mismatched interfaces and they can be modeled using the linear misfit dislocation density. The structures modeled in Fig. 1a exhibit at most 10 misfit dislocation regions (Dirac delta functions) which are equivalent with the number of mismatched interfaces. At low mismatch, the absence of peaks indicates that for layers near the surface, the strain energy is sufficient in relaxing the mismatch strain. However, at higher misfit strain, there exists a monotonic increase in the peak misfit dislocation density with increasing ending composition (mismatch), therefore necessitating the introduction of more misfit segments to relax the excess mismatch strain. In step-graded layers, the interfacial and surface misfit dislocation-free zones are limited by the growth step-size which, in this case, is one tenth of the buffer layer thickness. Figure 1b shows the equilibrium in-plane strain distribution for 500-nm thick $In_xGa_{1-x}As$ on GaAs (001) with various ending compositions. The in-plane strain profile comprises a series of step functions with discontinuities at the mismatched interfaces. Apart from the dislocated interfaces, the equilibrium strain in each sublayer is constant as expected. Correlating the results of Fig. 1a with b, it can be seen that the misfit dislocations relieve most of the excess strain associated with the compositional mismatch in sublayers near the interface, whereas the absence of dislocations near the surface results in higher residual elastic strain; in other words, for layers near the substrate interface, the in-plane strain is relatively small and does not change significantly from one layer to the next, whereas near the surface, the absence of peaks signify the major role of the strain energy in relaxing the local strain associated with the compositional mismatch. Furthermore, it can be seen from the results of Fig. 1b that the lowest mismatch shows the highest in-plane strain in the eighth and ninth steps, whereas in the final step the relation is reversed. The following is expected on the basis that at a low mismatch, both the strain and misfit dislocation energy play a major role in relaxing the misfit strain, whereas at higher mismatch, the misfit strain is mainly accommodated by the introduction of misfit dislocation. This phenomenon is also seen in the results of Fig. 1a where a low peak intensity or the absence of an MD peak indicates a noticeable contribution of the strain energy in relaxing the misfit strain (Fig. 1b). In the last step, the relation is reversed because it is energetically unfavorable for misfit dislocation to be introduced at the surface of the epilayer and, therefore, the misfit strain at the last step is accommodated by the strain energy. Experimental studies have also shown the absence of misfit dislocations[16,17] above the top step interface; in addition, the top step exhibits the maximum residual strain in the step-graded layer and the following holds with the deposition of each successive step.[16]

Figure 2a compares the average in-plane strain for $In_xGa_{1-x}As$ and $In_xAl_{1-x}As$ layers as a function of the average grading coefficient C_f where $C_f = f_h/h$. The results of Fig. 2a indicate a monotonic increase in the average in-plane strain in structures with a higher grading coefficient and smaller layer thickness. Moreover, structures with $In_xAl_{1-x}As$ as the epi-material exhibit greater average compressive strains (absolute valued) than $In_xGa_{1-x}As/GaAs$ (001). However, the curve separation between the two material systems becomes more prominent at higher grading coefficients and in structures with a smaller layer thickness. It is interesting to note that the strain–thickness product $\varepsilon_{||}h$ for both material systems is $\sim$2 nm. Although there is a slight dependence of the strain-thickness product $\varepsilon_{||}h$ on the elastic stiffness constants, the associated difference is within $\pm$0.1 nm. Even though the elastic stiffness constants are composition-dependent, the percent difference ΔC_{11} and ΔC_{12} with respect to the average value of both materials is given by

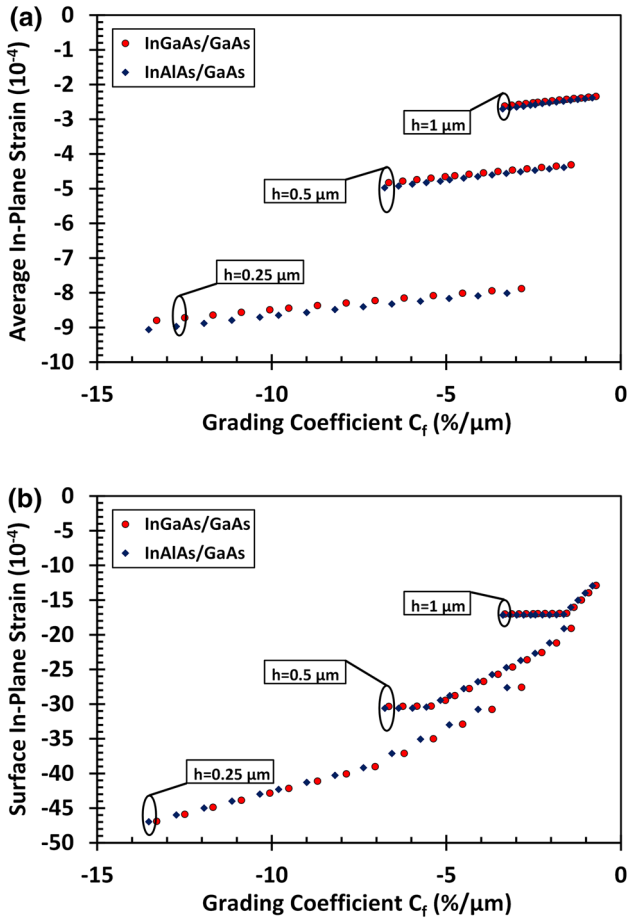

Fig. 2. (a) Average and (b) surface in-plane strain as a function of the grading coefficient for step-graded $In_xGa_{1-x}As/GaAs$ and $In_xAl_{1-x}As/GaAs$ heterostructures.

$$|\Delta C_{11}| = \left|\frac{C_{11,\mathrm{InAlAs}} - C_{11,\mathrm{InGaAs}}}{\frac{1}{2}\left(C_{11,\mathrm{InAlAs}} + C_{11,\mathrm{InGaAs}}\right)}\right| \times 100\% = \left|\left[0.17 - \frac{0.37}{3.17 - x}\right]\right| \times 100\%. \quad (3)$$

and

$$|\Delta C_{12}| = \left|\frac{C_{12,\mathrm{InAlAs}} - C_{12,\mathrm{InGaAs}}}{\frac{1}{2}\left(C_{12,\mathrm{InGaAs}} + C_{12,\mathrm{InGaAs}}\right)}\right| \times 100\% = \left|\left[\frac{0.2}{6.5 - x} - 0.04\right]\right| \times 100\%. \quad (4)$$

where x is the indium mole fraction. For the structures studied in this work, the percent difference in the material constants ΔC_{11} and ΔC_{12} ranges from 4.3 to 5.1% and 0.8 to 0.9%, respectively. The associated variation in the average in-plane strain due to the difference in the material constants ranges from approximately 4.3×10^{-6} to 2.7×10^{-5} corresponding to a percent difference of the in-plane strain in the range of 1.8–3%. Figure 2b compares the surface in-plane strain for $In_xGa_{1-x}As$ and $In_xAl_{1-x}As$ layers as a function of the average grading coefficient C_f. The surface in-plane strain exhibits a two-regime behavior; in regime one, the surface strain is monotonically increasing, whereas there exists a particular combination of ending indium composition and layer thickness (critical grading coefficient) where the surface strain exhibits saturation. This saturated value corresponds to the thickness of the individual steps and is associated with force balance on grown-in dislocations. The presence of dislocation peaks at the last mismatched interface indicates that the introduction of a misfit dislocation affords smaller energy budgets than relaxation via the strain energy. Below the critical grading coefficient, structures with $In_xGa_{1-x}As$ as the epilayer material contain a slightly higher compressive surface in-plane strain (absolute valued).

Experiments with $In_xAl_{1-x}As$ on GaAs substrates showed that step- and linearly graded layers exhibited similar values of surface in-plane strain[17] which allows the analysis above to indicate similar properties between the step- and linearly grading schemes. Furthermore, experimental investigation of step-graded layers involving a large number of steps has showed that the relaxation behavior approaches that of linearly graded buffers;[18] however, at low step numbers, these properties may be somewhat unique to step-graded layers. If we consider the force balance model on a grown-in dislocation, then the average residual strain in each step would be the same as that in a uniform layer with the same total thickness. Lynch et al. applied an *in situ* multibeam optical stress sensor to study the relaxation of $In_xAl_{1-x}As$ on a GaAs (001) substrate and showed that the deposition of each successive step gives rise to the relaxation of the underlying layers;[19] moreover, in order to maintain the $\varepsilon_{\|}h$ = constant relationship, the residual strain has to be concentrated in the top layer of the step-graded buffer. The results of Fig. 2b show that the top of the step-graded buffer is near fully relaxed in relatively thick layers. For step-graded layers with a thickness of $h = 250$nm and an ending mismatch varying from f_h = 0.8–3.4%, the percent relaxation in the top step ranged from 60% to 85%, respectively. In thicker structures, the percent relaxation in the top step is higher; for structures with a thickness of $h = 500$nm, the percent relaxation in the top step ranged from 73% to 91%, respectively, whereas in structures with a thickness of $h = 1000$nm, the percent relaxation in the top step ranges from 82% to 95%. This behavior has also been shown experimentally in $In_xGa_{1-x}As$ and $In_xAl_{1-x}As$ step-graded buffer layers; however, these structures involve the use of a thick device layer on top of the step-graded buffer. Jiang et al.[20] used high-resolution x-ray diffraction to study the relaxation of a multilayered structure composed of a 1-μm uniform layer of $In_{0.75}Al_{0.25}As$ grown on top of a GaAs substrate with an intermediate, 900-nm-

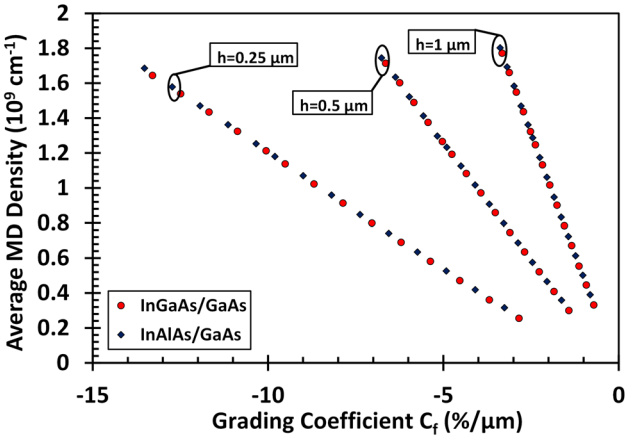

Fig. 3. Average misfit dislocation density as a function of the grading coefficient for step-graded $In_xGa_{1-x}As/GaAs$ and $In_xAl_{1-x}As/GaAs$ heterostructures.

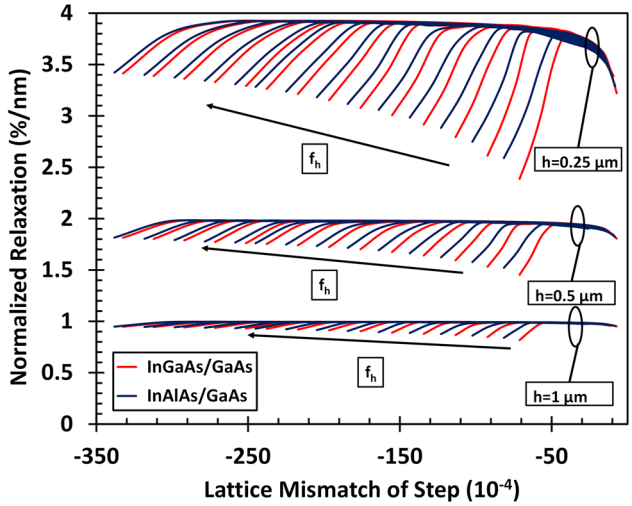

Fig. 4. Normalized relaxation percentage per unit thickness as a function of the ending lattice mismatch for step-graded $In_xGa_{1-x}As/GaAs$ and $In_xAl_{1-x}As/GaAs$ heterostructures. Each curve of a particular color represents an ending lattice mismatch value.

thick, step-graded (nine steps) layer of $In_xAl_{1-x}As$ with an indium composition ranging from 5% to 85%. Analysis of the x-ray rocking curves revealed that the device layer was near fully relaxed (98%) as a consequence of the overshoot design. In contrast, Shang et al.[21] showed 98% relaxation of the device layer in multilayered $In_xAl_{1-x}As$ structures without using an overshoot; however, the use of a thick step-graded buffer layer in this work resulted in a high degree of lattice relaxation in the device layer which removes the need for overshooting. Furthermore, Chen et al.[22] demonstrated 96% relaxation of the device layer in $In_xGa_{1-x}As$ multilayered structures.

The results of Fig. 3 indicate that there is an approximately linear and monotonic increase in the average equilibrium misfit dislocation density as a function of the average grading coefficient. In addition, an increase in the epilayer thickness yields higher dislocation densities. This behavior is expected on the basis that larger misfit strain requires the introduction of more misfit dislocation to relax the excess stress; moreover, for both material systems, the misfit dislocation introduction occurs at an approximate rate of 5.4×10^8 ($\% \times \text{cm}^{-1}$). Small differences in these two material systems are introduced by the difference in the elastic stiffness constants. Abrahams et al.[23] considered a simple model for step-graded layers and argued that the threading dislocation density would reach a steady-state value which depends on the average grading coefficient. Although threading dislocations are non-equilibrium defects, it can be argued that since each MD is associated with at most two threading dislocations and if we assume that the average length of misfit segments is fixed, then the steady threading dislocation density (and, therefore, the misfit dislocation density) at each step is proportional to the grading coefficient.

Figure 4 shows the normalized relaxation percentage per unit thickness as a function of the lattice mismatch at each step with the ending lattice mismatch as a parameter for $In_xGa_{1-x}As/GaAs$ (001) and $In_xAl_{1-x}As/GaAs$ (001) heterostructures. We define the normalized relaxation percentage per unit thickness of each step as:

$$|R_N| = \frac{f_N - \varepsilon_{||,N}}{h_N f_N} \times 100\%. \quad (5)$$

where f_N and $\varepsilon_{||,N}$ are the lattice mismatch and the in-plane strain of the step N, respectively, and h_N is the thickness of the step. We further define the normalized relaxation rate per unit thickness as the slope of the characteristic shown in Fig. 4. The results of Fig. 4 indicate a higher normalized relaxation rate per unit thickness in structures with a lower buffer layer thickness; this is expected on the basis that for the same ending composition, structures with a lower buffer thickness exhibit a higher grading coefficient and, therefore, require higher relaxation in accommodating the misfit strain. It can be seen that structures with lower ending indium composition and, therefore, mismatch contain higher relaxation rates near the surface and this phenomenon is associated with the absence of misfit dislocations, as shown on Fig. 1a. Moreover, there is an increase in the slope of the characteristic shown in Fig. 4 near the substrate interface with higher indium composition; however, the normalized relaxation rate per unit thickness becomes sluggish with increasing layer thickness. In comparison, for the same lattice mismatch profile, $In_xAl_{1-x}As/GaAs$ structures contain slightly higher misfit dislocation density (MDD) and, therefore, have a lower change in the normalized relaxation percentage from one mismatched interface to the other. Table I shows that for the heterostructures studied in this paper, an $In_xAl_{1-x}As/GaAs$ (001) material system exhibits higher elastic stiffness

coefficients. Combining the results of Figs. 2, 3 and 4, structures with $In_xAl_{1-x}As$ as the epilayer material exhibit higher average misfit dislocation densities and slightly higher average compressive in-plane strain (absolute valued), but contain a much lower rate of change in the normalized relaxation percentage per unit thickness of each step observable from the smaller slope values in Fig. 4.

CONCLUSION

We have investigated equilibrium lattice relaxation in metamorphic $In_xGa_{1-x}As/GaAs$ (001) and $In_xAl_{1-x}As/GaAs$ (001) heterostructures involving step-graded buffer layers. We have explored the equilibrium structure by studying the evolution of the misfit dislocation density and in-plane strain at the mismatched interfaces. The main conclusion to this paper is that structures with higher elastic stiffness coefficients such as an $In_xAl_{1-x}As/GaAs$ (001) material system exhibit greater average compressive in-plane strain (absolute valued) and misfit dislocations. In addition, the normalized relaxation rate per unit thickness at each step is determined by the misfit dislocation density at each mismatched interface. Equilibrium calculations are important when considering the kinetically limited relaxation of step-graded $In_xGa_{1-x}As/GaAs$ (001) and $In_xAl_{1-x}As/GaAs$ (001) structures, and understanding the misfit dislocation and in-plane strain distribution has important implications in the device design of semiconductor heterostructures.

REFERENCES

1. C.-S. Lee and W.-T. Chien, *J. Electrochem. Soc.* 158, H452 (2011).
2. H. Yang, H. Wang, and C.L. Tan, *IEEE Trans. Electron Dev.* 51, 1221 (2004).
3. J.-H. Tsai, *J. Electrochem. Soc.* 158, H889 (2011).
4. L.J. Mawst, J.D. Kirch, C.-C. Chang, T. Kim, T. Garrod, D. Botez, S. Ruder, T.F. Kuech, T. Earles, R. Tatavari, N. Pan, and A. Wibowo, *J. Cryst. Growth* 370, 230 (2013).
5. I. Mathews, D. O'Mahoney, A. Gocalinska, M. Manganaro, E. Pelucchi, H. Schmidt, A.P. Morrison, and B. Corbett, *Appl. Phys. Lett.* 102, 033906 (2013).
6. J. Tersoff, *Appl. Phys. Lett.* 62, 693 (1993).
7. J. Tersoff, *Appl. Phys. Lett.* 64, 2748 (1994).
8. E.A. Fitzgerald, Y.-H. Xie, D. Monroe, P.J. Silverman, J.M. Kuo, A.R. Kortan, F.A. Thiel, and B.W. Weir, *J. Vac. Sci. Technol. B* 10, 1807 (1992).
9. M.K. Hudait, Y. Lin, M.N. Palmisiano, and S.A. Ringel, *IEEE Electron Device Lett.* 24, 538 (2003).
10. T. Jian, W. Xiaoliang, and X. Hongling, *J. Semicond.* 35, 113006 (2014).
11. R. Suzuki, N. Taoka, M. Yokoyama, S. Lee, S.H. Kim, T. Hoshii, T. Yasuda, W. Jevasuwan, T. Maeda, O. Ichikawa, N. Fukuhara, M. Hata, M. Takenaka, and S. Takagi, *Appl. Phys. Lett.* 100, 132906 (2012).
12. S. Kim, M. Yokoyama, N. Taoka, R. Iida, S. Lee, R. Nakane, Y. Urabe, N. Miyata, T. Yasuda, H. Yamada, N. Fukuhara, M. Hata, M. Takenaka, and S. Takagi, *Appl. Phys. Express* 4, 02420 (2011).
13. M.S. Leite, R.L. Woo, J.N. Munday, W.D. Hong, S. Mesropian, D.C. Law, and H.A. Atwater, *Appl. Phys. Lett.* 102, 033901 (2013).
14. H. Roehle, R.J.B. Dietz, H.J. Hensel, J. Böttcher, H. Künzel, D. Stanze, M. Schell, and B. Sartorius, *Opt. Express* 18, 2296 (2010).
15. B. Bertoli, E.N. Suarez, J.E. Ayers, and F.C. Jain, *J. Appl. Phys.* 106, 073519 (2009).
16. G. Salviati, C. Ferrari, L. Lazzarini, S. Franchi, A. Bosacchi, F. Taiariol, M. Mazzer, C. Zanotti-Fregonara, F. Romanato, and A.V. Drigo, *Inst. Phys. Conf. Ser.* 146, 337 (1995).
17. D. Lee, M.S. Park, Z. Tang, H. Luo, R. Beresford, and C.R. Wie, *J. Appl. Phys.* 101, 063523 (2007).
18. F. Capotondi, G. Biasiol, D. Ercolani, V. Grillo, E. Carlino, F. Romanato, and L. Sorba, *Thin Sol. Films* 484, 400 (2005).
19. C. Lynch, R. Beresford, and E. Chason, *J. Vac. Sci. Technol. B* 22, 1539 (2004).
20. Z. Jiang, W. Wang, H. Gao, L. Liu, H. Chen, and J. Zhou, *Appl. Surf. Sci.* 254, 5241 (2008).
21. X.Z. Shang, S.D. Wu, C. Liu, W.X. Wang, L.W. Guo, and Q. Huang, *J. Phys. D* 39, 1800 (2006).
22. J. Chen, J.M. Fernandez, J.C.P. Chang, K.L. Kavanagh, and H.H. Wieder, *Semicond. Sci. Technol.* 7, 601 (1992).
23. M.S. Abrahams, L.R. Weisberg, C.J. Buiocchi, and J. Blanc, *J. Mater. Sci.* 4, 223 (1969).